


Sclerostin Downregulation Globally by Naturally Occurring Genetic Variants, or Locally in Atherosclerotic Plaques, Does Not Associate With Cardiovascular Events in Humans

Gill Holdsworth,¹  James R Staley,¹ Peter Hall,¹ Ian van Koevorden,² Ciara Vangjeli,¹ Remi Okoye,¹ Rogely W Boyce,³ James R Turk,³ Martin Armstrong,⁴ Alison Wolfreys,¹ and Gerard Pasterkamp²

¹UCB Pharma, Slough, UK

²University Medical Centre Utrecht, Utrecht, The Netherlands

³Amgen Inc., Thousand Oaks, CA, USA

⁴UCB Pharma, Braine-L'Alleud, Belgium

ABSTRACT

Inhibition of sclerostin increases bone formation and decreases bone resorption, leading to increased bone mass, bone mineral density, and bone strength and reduced fracture risk. In a clinical study of the sclerostin antibody romosozumab versus alendronate in postmenopausal women (ARCH), an imbalance in adjudicated serious cardiovascular (CV) adverse events driven by an increase in myocardial infarction (MI) and stroke was observed. To explore whether there was a potential mechanistic plausibility that sclerostin expression, or its inhibition, in atherosclerotic (AS) plaques may have contributed to this imbalance, sclerostin was immunostained in human plaques to determine whether it was detected in regions relevant to plaque stability in 94 carotid and 50 femoral AS plaques surgically collected from older female patients (mean age 69.6 ± 10.4 years). Sclerostin staining was absent in most plaques (67%), and when detected, it was of reduced intensity compared with normal aorta and was located in deeper regions of the plaque/wall but was not observed in areas considered relevant to plaque stability (fibrous cap and endothelium). Additionally, genetic variants associated with lifelong reduced sclerostin expression were explored for associations with phenotypes including those related to bone physiology and CV risk factors/events in a population-based phenome-wide association study (PheWAS). Natural genetic modulation of sclerostin by variants with a significant positive effect on bone physiology showed no association with lifetime risk of MI or stroke. These data do not support a causal association between the presence of sclerostin, or its inhibition, in the vasculature and increased risk of serious cardiovascular events. © 2021 The Authors. *Journal of Bone and Mineral Research* published by Wiley Periodicals LLC on behalf of American Society for Bone and Mineral Research (ASBMR).

KEY WORDS: BONE MINERAL DENSITY; CARDIOVASCULAR; GENETICS; PHENOMEWIDE ASSOCIATION STUDY; SCLEROSTIN; SOST

Introduction

Sclerostin is the secreted protein product of the *SOST* gene, which inhibits canonical Wnt signaling in the skeleton, acting as a negative regulator of bone formation.⁽¹⁾ Genetic deficiency or absence of sclerostin causes the rare high bone mass conditions sclerosteosis and van Buchem disease.^(2,3) In adults, sclerostin is principally expressed by skeletal osteocytes.⁽⁴⁾ Inhibition of sclerostin increases bone formation and decreases bone resorption, leading to increased bone mass, bone mineral density (BMD), and bone strength and reductions in fracture risk.^(5,6)

SOST mRNA/sclerostin protein is also constitutively expressed in aorta^(3,7–9) and upregulated in foci of vascular calcification.^(10–15) The function of sclerostin in the vasculature is unclear; however, it has been previously proposed as a potential inhibitor of vascular calcification.^(10,15) Since excess sclerostin has been reported to be protective against atheroprotection and inflammation in an ApoE mouse model,⁽⁹⁾ it has also been hypothesized that a reduction in sclerostin could be associated with an increased risk of atheroprotection. However, a recently published study found no association between sclerostin inhibition and atheroprotection when reduction in sclerostin was directly assessed in two ApoE mouse models using different methods of inducing

This is an open access article under the terms of the Creative Commons Attribution-NonCommercial-NoDerivs License, which permits use and distribution in any medium, provided the original work is properly cited, the use is non-commercial and no modifications or adaptations are made.

Received in original form December 2, 2020; revised form March 4, 2021; accepted March 7, 2021; Accepted manuscript online March 19, 2021.

Address correspondence to: Gill Holdsworth, PhD, UCB Pharma, 208 Bath Road, Slough SL1 3WE, UK. E-mail: gill.holdsworth@ucb.com

Additional Supporting Information may be found in the online version of this article.

Journal of Bone and Mineral Research, Vol. 36, No. 7, July 2021, pp 1326–1339.

DOI: 10.1002/jbmr.4287

© 2021 The Authors. *Journal of Bone and Mineral Research* published by Wiley Periodicals LLC on behalf of American Society for Bone and Mineral Research (ASBMR).

atheroprogession.⁽¹⁶⁾ In the recent ARCH phase III comparator clinical trial of the sclerostin antibody romosozumab or alendronate in women with postmenopausal osteoporosis, a numerical imbalance in positively adjudicated serious cardiovascular adverse events was observed during the first 12 months of the study (50 patients [2.5%] in the romosozumab group versus 38 patients [1.9%] in the control alendronate group),⁽¹⁷⁾ which was driven by a greater number of myocardial infarction and stroke events. Thus, the aim was to explore whether there was any credible association between sclerostin expression in the vasculature and cardiovascular outcomes that could indicate a potential biological plausibility between sclerostin inhibition and the reported imbalance in cardiovascular (CV) events (myocardial infarction [MI] and stroke). Atherosclerosis is a chronic progressive inflammatory disease of the arterial wall that is a significant cause of morbidity and mortality.⁽¹⁸⁾ Sudden changes in advanced atherosclerotic (AS) plaques, such as plaque erosion or rupture with thrombosis or arterial spasm in the presence or absence of plaque,^(19,20) are common pathological mechanisms associated with adverse cardiovascular events such as MI and stroke. Plaque rupture is usually associated with the “vulnerable” plaque morphology.⁽²¹⁾ However, superficial erosion of fibrous plaques, which is more frequently observed in women, is recognized as a significant driver of acute coronary deaths.^(22–24)

Little is known about sclerostin expression in AS plaques. Here, immunohistochemistry (IHC) was used to assess sclerostin expression in advanced AS plaques collected from older female patients and stored in the AtheroExpress biobank.⁽²⁵⁾ This enabled assessment of sclerostin expression in the atherosclerotic plaques in women of a similar age range to those who may be considered for treatment with sclerostin-neutralizing antibodies and any potential association between sclerostin staining and histological features of plaque instability, intra-plaque cytokine profile, or patient demographics: age at endarterectomy, history of arterial disease pre-surgery, or cardiac events during a 3-year follow-up period.

To further explore any mechanistic links between reduced sclerostin and cardiovascular outcomes, population-based genetic approaches were employed. Phenomewide association studies (PheWAS) allow unbiased, systematic assessment of causative associations between common human genetic variants and multiple human diseases and phenotypic traits.⁽²⁶⁾ Although the effect sizes of complex trait genetic associations tend to be small in magnitude⁽²⁷⁾ (especially when compared with drug effects), this approach allows naturally occurring common genetic variation within a population to be used as a surrogate for the action of a drug, providing supporting data to predict both efficacy and on-target safety profiles.^(28,29) Here, variants in the *SOST* region associated with reduced expression of the *SOST* gene, encoding sclerostin, and increased BMD were selected as a proxy for sclerostin inhibition and used in PheWAS to assess the phenotypic associations for these variants at a population level. Implicitly, if the variants reflect the pharmacological action of sclerostin inhibition, then associations with increased BMD and reduced risk of fractures would be expected. Therefore, the same variants can be used to explore any mechanistic link between genetically reduced sclerostin levels and cardiovascular outcomes.

Materials and Methods

Immunohistochemistry of atherosclerotic plaques

Comparison of sclerostin antibody specificity

Four-micrometer sections were freshly cut from formalin-fixed paraffin-embedded (FFPE) blocks, mounted onto SuperFrost

Ultra Plus GOLD adhesion slides (Thermo Fisher Scientific, Waltham, MA, USA), and dried overnight in a 37°C oven. The two proprietary Scl-Abs, Scl-Ab #1 and Scl-Ab #2, were each used at 1:1000 and two commercially available Scl-Abs, ab63097 (Abcam, Cambridge, MA, USA) and ab75914 (Abcam) (referred to as Scl-Ab #3 and #4) were used at 1:900 and 1:50, respectively. The mouse and rabbit isotype-matched control antibodies were diluted to give a similar protein concentration to the sclerostin antibodies. Staining was performed using a BOND RX fully automated research stainer (Leica Biosystems, Wetzlar, Germany) with 20-minute antigen retrieval (pH 6) and 30-minute incubation with primary antibody. Hematoxylin counterstain was included in all four IHC protocols.

Study design and population

A subset of carotid and femoral/iliac artery plaques from female patients showing 50% to 95% stenosis who had given informed consent for collaboration with external private partners were selected from the AtheroExpress biobank for the current study.

Positive control tissues included human aorta (one in transverse section and one in longitudinal section) and decalcified bone from cynomolgus monkey (a species known to express sclerostin in osteocytes).⁽¹⁶⁾ The control cynomolgus bone tissue came from archived material left over from an unrelated study conducted at SNBL in Japan in 2008. Ethical approval was from the SNBL IACUC. Samples were shipped to the UK in 2010 with CITES certification. Human kidney and liver do not express sclerostin protein so they were chosen as suitable negative control tissues.

Staining of histological sections

Serial transverse sections (3 µm) were freshly cut from FFPE blocks, mounted onto Surgipath X-tra Adhesive micro slides (Leica Biosystems) and maintained at 4°C before staining with Scl-Ab #1 (diluted 1:250; approximately 15 µg/mL) or isotype-matched control antibody (diluted to give a similar protein concentration to sclerostin antibody). Alpha smooth muscle actin antibody (αSMA), Sigma (St. Louis, MO, USA) clone 1A4, was used at 1:32,000. Staining was performed using Ventana Benchmark Ultra with 12-minute antigen retrieval (EDTA) and 32-minute incubation with primary antibody. Hematoxylin counterstain was included in all three IHC protocols.

Visualization and evaluation of stained sections

After IHC staining, slides were visualized under light microscopy by the study pathologist for expression of sclerostin protein. The study pathologist judged each slide for adequacy and quality of tissue elements and specificity of staining before assessing sclerostin expression within each plaque. The intensity, percentage circumference of staining, and region of staining were assigned as applicable.

Interpretation was based on comparisons to physiologic/expected sclerostin expression and staining patterns/histologic locations within positive control aorta samples. The presence of granular deposits arranged in a linear or semi-linear pattern, parallel to stromal elements, was considered positive sclerostin staining, consistent with a secreted protein from vascular smooth muscle cells (VSMCs). Non-specific staining was associated with section lifting/folding and often produced characteristic geometric patterns distributed randomly within the sample. Sclerostin, αSMA, and hematoxylin and eosin (H&E) slides for

each tissue were reviewed by the study pathologist. These were used for adjunctive comparison with the sclerostin IHC-stained slides and to identify histological features within the plaques.

Sclerostin IHC scoring

Two positive control aorta samples were scored for staining intensity. One transverse aorta section was scored for circumferential percentage staining, whereas only location and staining characteristics were described for the other longitudinal section. All plaque samples were scored for sclerostin staining intensity, circumferential percentage staining, and, for the tunica intima (T. intima) only, location of staining (superficial, mid, or deep) using the following criteria:

- Intensity of staining was scored semi-quantitatively on a scale of 0 to 4 where: 0 = no staining; 1 = minimal pale staining that could clearly be distinguished from non-specific background staining; 2 = mild staining that was more intense than minimal; 3 = moderate staining that was more intense than mild; 4 = severe staining that was similar in intensity noted in positive control aorta samples and of dark brown-black coloration.
- Circumferential staining was scored semi-quantitatively to the nearest whole unit of 10 as a percentage of total circumference identified under low-power magnification. Where staining was <10%, this was indicated as an approximate % score and/or described in the comments.
- In the T. intima, staining location was scored on the following five levels: level 1 = superficial plaque/T. intima in area of plaque cap; level 2 = mid region of plaque between levels 1 and 3; level 3 = deep plaque/T. intima adjacent to T. media; level 4 = mid and deep region of plaque/T. intima (ie, level 2 and level 3); level 5 = superficial, mid, and deep region of plaque/T. intima.

Integration of sclerostin staining with AtheroExpress biobank data

Because of the relatively small number of samples showing sclerostin staining, the cohort was dichotomized into two groups: one group without sclerostin staining and one group with sclerostin staining. Analyses included the proportion of plaques in which sclerostin expression was observed in relation to baseline patient characteristics, namely age at endarterectomy and recorded history of coronary artery disease or peripheral artery disease. The association of sclerostin staining with the major adverse cardiovascular event (MACE: stroke, myocardial infarction, or cardiovascular death) endpoint was also examined.

Human genetic analyses

SOST genetic variant selection

To select genetic variants that mimic *SOST* inhibition, variants associated with lower mRNA *SOST* expression were chosen. All variants that satisfied the following criteria were eligible for selection:

- Associated with mRNA *SOST* expression in tibial artery or heart tissue in GTEx v8^(30,31) (as cardiovascular endpoints are of interest here and as bone is not included in GTEx) at genome-wide significance level (5×10^{-8})⁽³¹⁾
- Associated with BMD levels, estimated using heel ultrasound, at genome-wide significance level⁽³²⁾
- Within ± 100 kb of the *SOST* gene

These eligible variants (of which there were 99) were then linkage disequilibrium (LD) pruned using LDlink (r^2 cut-off of 0.2)⁽³³⁾ using the European samples from 1000 Genomes, a whole-genome sequencing project commonly used in the genetics field to compute LD statistics, as the LD reference panel.⁽³⁴⁾ The same variants were selected if the analysis was restricted to tibial artery only and if results from all tissues in GTEx v8 were used.

Two additional strategies were used to select variants related to reduced sclerostin levels. The first are variants that are associated with circulating sclerostin protein levels at genome-wide significance level (rs215226 and rs7241221)⁽³⁵⁾ and the second are two variant sets associated with BMD levels in the *SOST* region (rs7209826 and rs188810925; rs2741856 and rs7217502) found in recent large-scale genome-wide association studies.^(32,36) The correlations between the variants in these variant sets are displayed in Supplemental Fig. S4.

Correlation statistics between *SOST* variants, ie, LD statistics, were computed using the European samples from 1000 Genomes.⁽³⁴⁾ The measures computed were r (similar to Pearson's correlation coefficient) and D' .⁽³⁷⁾ A chi-square test of independence (for a 2×2 table) was used to assess the relationship between two variants.

Phenome-wide association study

The PheWAS was performed using look-ups from the latest UK Biobank genetic analyses (mean age = 56.5 years and proportion of males = 46.2%) from the Neale Lab (www.nealelab.is/uk-biobank/ and Sudlow and colleagues)⁽³⁸⁾ and PhenoScanner,^(39,40) as well as from additional data sets related to bone physiology and cardiovascular disease and risk factors.^(32,41-47) For completeness, the variants were also queried in the GWAS catalog⁽⁴⁸⁾ and IEU GWAS server,⁽⁴⁹⁾ but no additional relevant associations were identified. The full list of studies used in the present analysis is available in Supplemental Table S10. Of particular interest are those data sets related to bone physiology and cardiovascular disease. The genetic associations with these phenotypes were studied in large population-based studies: GEFOS (bone mineral density, $N = 426,824$, fracture risk cases/controls = 53,184/373,611),⁽³²⁾ CARDIoGRAMplusC4D (coronary artery disease cases/controls = 122,733/424,528,⁽⁴⁶⁾ myocardial infarction cases/controls = 43,676/128,199),⁽⁴⁴⁾ and MEGASTROKE (all stroke cases/controls = 67,162/454,450, ischemic stroke cases/controls = 60,341/454,450).⁽⁴²⁾

To ensure that one association is included in the analysis for each variant-phenotype pair, we selected a single result for each pair based on the largest number of cases for binary phenotypes and the largest number of samples for continuous phenotypes. All phenotypes were categorized into one of the following phenotypic categories: anthropometric, behavioral, cancer and neoplasms, circulatory, dermatologic, digestive, endocrine and metabolic, genitourinary and reproductive, hematopoietic, immune system, infectious, musculoskeletal, neurological, psychiatric, respiratory, and sensory.

Conditional analyses

Because there is a well-known genetic association between *CD300LG* and triglyceride and HDL levels in the *SOST* gene region, we used conditional analyses to adjust for genetic variations related to *CD300LG*. As apolipoprotein A is highly correlated with HDL levels (genetic correlation = 0.92),⁽⁵⁰⁾ we also adjusted these associations for variations related to *CD300LG*. These conditional analyses were performed using the COJO

methodology,⁽⁵¹⁾ which allows variant effects to be adjusted for each other using summary level results. The European samples from 1000 Genomes were used as the LD reference panel.⁽³⁴⁾ If a nominal association of $p < .001$ (at the PheWAS level) was observed for at least one of these lipid measures with a *SOST* variant, these associations for this variant were either adjusted for rs72836561 (missense variant in *CD300LG*) or rs72836567 (downstream of *CD300LG* and the top associated variant with mRNA *CD300LG* expression),⁽³⁰⁾ where the choice of *CD300LG* variant was based on the correlation structure with the *SOST* variant.

Meta-analysis of allelic effects

Effects across variants were meta-analyzed for key clinical endpoints and risk factors using fixed-effects meta-analysis accounting for any residual correlation between the variants.^(52,53) This model is a weighted generalized linear regression of the form $\hat{\beta}_{MA} = (\mathbf{1}^T \Omega^{-1} \mathbf{1})^{-1} \mathbf{1}^T \Omega^{-1} \hat{\beta}$ and $SE(\hat{\beta}_{MA}) = \sqrt{(\mathbf{1}^T \Omega^{-1} \mathbf{1})^{-1}}$, where $\hat{\beta}$ is the vector of variant-phenotype estimates, $\mathbf{1}$ is an intercept vector, and $\Omega = \sigma \sigma^T \circ \rho$, where σ is the vector of corresponding standard errors of $\hat{\beta}$ and ρ is the variant correlation matrix. The genotype correlation statistics between the variants (that make up ρ) were computed using the European samples from 1000 Genomes.⁽³⁴⁾

Statistical analysis

For the immunohistochemistry study, both histological plaque features and subsequent cardiovascular events were tested for an association with sclerostin staining using Pearson chi-square test. A linear regression model was used to test for a linear relationship between sclerostin staining and the concentration of cytokines (IL6, MCP1, TNF α) and osteopontin (OPN) measured in plaque. These cytokines were selected based on the availability of preexisting data in the AtheroExpress biobank. These statistical analyses were performed using SPSS version 21.0 (SPSS Inc., Chicago, IL, USA) and a p value of $< .05$ was considered significant.

For the human genetic analyses, in PheWAS, many variant-phenotype associations were tested, therefore a Bonferroni adjusted p value of .05 divided by the number of tests performed was used to account for multiple testing (eg, in the primary analysis of variants associated with *SOST* mRNA expression, the threshold = $0.05/4887 \approx 1.0 \times 10^{-5}$).⁽⁵⁴⁾ All associations with binary phenotypes on the risk difference scale were transformed to the odds ratio scale.⁽⁵⁵⁾ In the analysis of cardiovascular endpoints and risk factors, 18 phenotypes were assessed, therefore a Bonferroni-adjusted p value threshold of $0.05/18 = 0.0028$ was used. The genetic data processing and analyses were performed using python version 3.6 (package: pandas),⁽⁵⁶⁾ R version 3.6 (packages: ggplot2,⁽⁵⁷⁾ pheatmap, and metafor),⁽⁵⁸⁾ and tabix.⁽⁵⁹⁾

Study approval

Carotid and femoral/iliac artery plaques from the AtheroExpress biobank were collected from patients who had given written informed consent as previously described;⁽²⁵⁾ only plaques from patients who had given informed consent for collaboration with external private partners were selected for the current study.

All the participants in the UK Biobank, GEFOS, CARDIoGRAM-plusC4D, and MEGASTROKE cohorts provided written informed consent for participating in research studies. Blood or saliva samples were collected according to protocols approved by local

institutional review boards. Details are provided in the original publications describing the cohorts.^(32,38,42,44,46)

Results

Immunohistochemistry of atherosclerotic plaques

Plaque characteristics

We selected a random sample of 94 carotid and 50 femoral/iliac artery plaques acquired from female patients of an age that meant they were likely to be postmenopausal (mean age 69.6 years \pm 10.4), and archived as FFPE blocks in the AtheroExpress biobank. The characteristics of the study group are summarized in Supplemental Table S1.

Plaques had been collected during surgical endarterectomy from patients showing 50% to 95% stenosis. In this procedure, the plaque and adjacent T. intima was dissected away leaving a significant proportion of samples with residual tunica media (T. media), confirmed by H&E and α SMA staining. T. media was present in 97% of carotid artery plaques and 78% of femoral/iliac samples. Plaques were classified as previously described.⁽²⁵⁾ Carotid plaques were categorized as atheromatous (33%), fibroatheromatous (16%), or fibrous (51%), whereas femoral/iliac plaques were typically fibrous (88%) with the remainder being fibroatheromatous.

Sclerostin antibody optimization and specificity

Careful optimization of the sclerostin IHC protocol was critical to ensure the specificity of staining and hence the reliability and reproducibility of this study. Two proprietary sclerostin antibodies (Scl-Ab) and two commercially available Scl-Ab were evaluated for their ability to sensitively and specifically stain sclerostin protein in FFPE tissue sections. In GTEx v8,⁽³⁰⁾ human aorta is the tissue with the highest expression of *SOST* mRNA (note that bone is not included in GTEx) so it was used as a positive control tissue. Human kidney and liver were chosen as negative control tissues; kidney expresses *SOST* mRNA^(2,3) but not sclerostin, whereas *SOST* is not detected in liver.⁽²⁾

All four Scl-Ab tested showed strong staining of VSMC in aorta T. media; however, three of the four antibodies exhibited non-specific (background) staining in the negative control kidney and liver sections, where sclerostin is not expressed (Supplemental Fig. S1), thus their use would generate misleading data on tissue protein expression. Only one antibody (Scl-Ab #1) showed specific and sensitive staining of positive control tissues and absent staining of the negative control section and hence was suitable for IHC applications. This antibody was used to stain the 144 AS plaques selected from the AtheroExpress biobank.

Sclerostin expression in normal aorta and atherosclerotic plaques from the AtheroExpress biobank

Using an optimized sclerostin staining protocol for the selected antibody, intense sclerostin immunoreactivity was observed in decalcified cynomolgus bone, which was similar to that previously reported in human bone,⁽⁴⁾ and in two control FFPE normal aorta specimens, whereas an isotype negative control antibody showed no staining, demonstrating high specificity of staining for sclerostin (Supplemental Fig. S2). Fig. 1A

shows intense extracellular sclerostin-positive granular staining in the stroma of the T. media, forming a linear pattern that tended to align parallel to elastin laminae. Sclerostin staining

was discontinuous and occupied approximately 30% of the circumference of the aorta. In contrast to the robust sclerostin staining observed in the T. media of normal human aorta, most (67%) plaques were negative for sclerostin immunoreactivity (presented in detail below) and when present, sclerostin staining in AS plaques was weaker and more variable compared with non-diseased aorta. When sclerostin was detected in plaques, staining was predominantly minimal to mild (semi-quantitative score of 1 to 2) and typically occupied up to a third of the circumference of the vessel wall compared with intense (semi-quantitative score of 4) in positive control aorta sections. Sclerostin immunoreactivity was predominantly found in T. media and sometimes extended into the immediate adjacent subintima (representative image shown in Fig. 1B). Sclerostin staining of the subintima also generally occupied up to 30% of the vessel wall circumference and was predominantly minimal to mild in intensity (again, reduced intensity compared with control aorta samples). Staining was predominantly extracellular and characterized by granular staining of matrix elements, which formed a linear pattern aligned along matrix fibers. Cell bodies of smooth muscle cells were not distinct, but when visible

appeared as weak granular cytoplasmic sclerostin expression. Occasionally more intense granular staining was visible, often oriented in a perinuclear location (Fig. 1C). Importantly, sclerostin staining was never observed in the overlying superficial T. intima, luminal endothelium, associated inflammatory cells (representative image shown in Fig. 1D), or within the mineralized/necrotic core of the plaque. Fig. 1E shows a diagram summarizing the typical location of sclerostin staining in the plaques assessed in this study. Of the plaques surveyed, 67% (97/144) were judged to be negative for sclerostin staining. Fifteen plaques demonstrated staining of both T. media and T. intima (which was always the adjacent subintima), whilst staining of only T. media or only T. intima (which was always deeper regions of subintima distant from the lumen) was recorded in 14 and 18 plaques, respectively. T. media was judged to be absent in 14 of the 144 plaques hence those plaques were not scored for T. media staining. As shown in Fig. 2A, the frequency of sclerostin staining was higher in plaques dissected from the carotid artery compared with those removed from the femoral/iliac arteries (42% versus 16%, respectively). When the location of sclerostin within the plaque was considered, T. media staining was recorded in 29% of carotid plaques

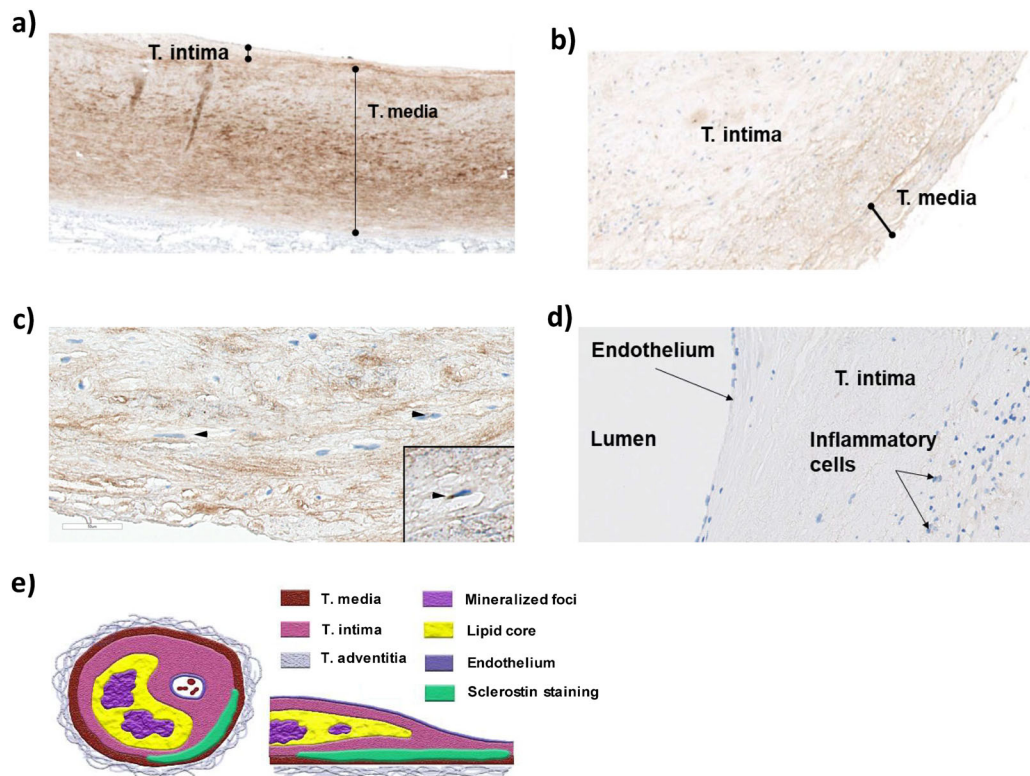


Fig 1. Representative sclerostin staining in human aorta and advanced human atherosclerotic (AS) plaques. (A) Intermediate-power photomicrograph showing intense sclerostin staining in human aorta. Note the strong granular/linear staining within the T. media of the aorta oriented parallel to elastin laminae. (B) Intermediate-power photomicrograph showing mild sclerostin staining in the T. media and immediate adjacent overlying subintima of an advanced human AS plaque. (C) High-power image of T. media from an atherosclerotic plaque that showed moderate sclerostin expression. Staining was predominantly extracellular and was characterized by granular staining of matrix elements that formed a linear pattern aligned along matrix fibers. Cell bodies of smooth muscle cells (arrowheads) were not distinct, but when visible appeared as weak granular cytoplasmic sclerostin expression. Occasionally more intense granular staining was visible, often orientated in a perinuclear location. Inset image shows a digitally magnified smooth muscle cell taken from another field showing intense perinuclear staining of presumptive Golgi apparatus. (D) Intermediate-power photomicrograph showing absence of sclerostin staining in superficial region, endothelium, and adjacent inflammatory cells in advanced AS plaque. (E) Schematic representation showing histological features of advanced AS plaque and distribution of observed sclerostin staining in transverse and longitudinal section.

versus 8% of femoral/iliac, whereas the frequencies for T. intima staining were 29% versus 12% in carotid and femoral/iliac plaques, respectively. Because of the relatively low rate of sclerostin staining observed, most subsequent analyses were performed after dichotomization into “sclerostin staining” or “no sclerostin staining,” based on the simple presence or absence of staining of either T. media or T. intima.

The risk of major adverse cardiovascular events (stroke, myocardial infarction, or cardiovascular death) increases with age.^(60–62) To assess the influence of age on sclerostin staining or endarterectomy location, sclerostin staining was stratified for comparison in women younger than 75 or 75 years and older at the time of endarterectomy. Of the total cohort, 63% (91/144) were in the younger group (mean age 63.7 ± 8.2 years, median 67 years), whereas the remaining 37% (53/144) were aged 75 years and older (79.8 ± 3.7 years, median 79 years). The frequency of sclerostin staining in plaques was similar between the age groups (Fig. 2B). Approximately half (52/91; 57%) of carotid artery plaques originated from patients younger than 75 years of age at the time of surgery and there was no difference in the proportion of carotid artery plaques staining for sclerostin expression by age grouping (42% and 40% for younger and older groups, respectively). In contrast, plaques were more frequently collected from the femoral/iliac arteries of patients in the younger cohort (39/50; 78%) and sclerostin expression was slightly more frequently observed in these samples: 18% compared with 9% staining positive for the older group. Overall, there was no indication of an association between sclerostin staining (presence or absence) and patient age at endarterectomy.

Sclerostin staining association with plaque characteristics and cardiac clinical outcomes

Changes in AS plaque composition have been linked to thrombotic events and thus to clinical outcome.^(63,64) The relationship between the sclerostin staining and various features that describe the phenotype and stability of the plaque was assessed (namely intraplaque hemorrhage, lipid content, smooth muscle cells, collagen, and calcification; data summarized in Supplemental Table S2). None of these features showed a statistically significant association with the detection of sclerostin, apart from dystrophic calcification of the acellular necrotic core of plaques, which was inversely correlated with sclerostin staining ($p < .05$).

In an ApoE mouse model of atherosclerosis, elevated sclerostin reduced circulating levels of the pro-inflammatory cytokines MCP1, IL6, and TNF α ,⁽⁹⁾ whereas elevation of osteopontin (OPN) in human carotid and femoral plaques was identified as a predictive outcome marker of cardiovascular events.⁽⁶⁵⁾ This raised the question whether reduced sclerostin would lead to increased pro-inflammatory cytokine levels and/or alter OPN levels. In the current study, there was no linear relationship between sclerostin staining of T. intima or T. media and the expression of MCP1, IL6, and TNF α or OPN within the subset of plaques for which this data was available (Supplemental Table S3).

Finally, the clinical history and follow-up data on file were tested for association with patient-reported arterial disease before endarterectomy. Coronary artery disease (CAD) was recorded in 31% of the total cohort (45/143; data for one patient was not available), which represented 26% of the carotid artery samples and 42% of the femoral/iliac plaques. Peripheral artery disease (PAD) was noted in 40% (57/143) of the total cohort; the majority (47) of these samples originated from the femoral/iliac group. The presence of arterial disease at surgery did not appear to be associated with sclerostin expression because there

was no significant difference in the frequency of positive sclerostin staining in plaques collected from patients with CAD or PAD compared with the total cohort (Fig. 2C). MACE (stroke, myocardial infarction, or cardiovascular death) occurred in 15% (21/144) of patients during the 3-year follow-up period, with similar rates observed for the carotid and femoral/iliac cohorts (16% in the carotid group versus 12% in the femoral/iliac group). There was no significant association between sclerostin staining and whether MACE was reported during the 3-year follow-up period (Fig. 2D).

Human genetic analyses

To further explore whether a mechanistic lowering of sclerostin levels was associated with increased cardiovascular risk, a comprehensive PheWAS was performed. This population level assessment explored whether individuals with lifelong genetically lowered sclerostin expression were at increased risk of cardiac-related outcomes (see Materials and Methods). Variants associated with both reduced *SOST* mRNA expression in artery and increased BMD (three variants), or which had been previously associated with reduced circulating sclerostin protein and increased BMD (two variants), were used as a surrogate for non-saturating sclerostin inhibition.^(17,66,67) To further explore the validity of the inferences from these variants, four additional variants in the *SOST* region that are associated with BMD were assessed in sensitivity analyses.

Exploration of phenotypes of genetic variants associated with reduced SOST expression and sclerostin levels

Three common genetic variants (frequency of the minor allele >5%) associated with reduced mRNA expression of *SOST* in arteries in GTEx v8⁽³⁰⁾ were selected to represent variation across the *SOST* locus; these were rs9899889, rs1107748, rs66838809 (Supplemental Fig. S3 and Supplemental Table S4); see Materials and Methods for detailed selection criteria). These variants cover the three main linkage disequilibrium blocks associated with *SOST* mRNA expression in the region (Supplemental Fig. S4). Alleles associated with lower *SOST* expression in artery (p values ranging from 7.30×10^{-11} to 2.80×10^{-40}) were positively associated with BMD (overall effect 0.026 [95% confidence interval (CI) 0.023–0.028; $p = 1.02 \times 10^{-70}$; $n = 426,824$], Supplemental Fig. S5) and reduced fracture risk (overall effect odds ratio 0.968 (95% CI 0.959–0.978; $p = 3.20 \times 10^{-10}$; cases/controls = 53,184/373,611), Supplemental Fig. S5), thereby indicating a biological outcome consistent with sclerostin pharmacology. Although these variants were strongly associated with multiple skeletal-related phenotypes (eg, heel and spine bone mineral density, fracture incidence, standing height), there was no evidence for association of any variants with ischemic or other cardiovascular events after correction for multiple testing (Fig. 3A and Supplemental Table S5; Bonferroni p -value threshold = .05/number of tests performed $\approx 1 \times 10^{-5}$, shown as a dotted line). rs9899889 was associated with lower triglyceride levels and higher HDL cholesterol and apolipoprotein A levels (Supplemental Table S6). There is a known genetic association with these lipid measures with the nearby *CD300LG* gene,^(68–75) in particular with its missense variant rs72836561, and after adjusting the rs9899889 lipid results for rs72836561, there were no longer any significant associations (all p values >.05; Supplemental Table S6). Moreover, with this adjustment, the associations with cardiovascular phenotypes are in line with what would be expected by chance, with all the circulatory associations either falling within or nearby

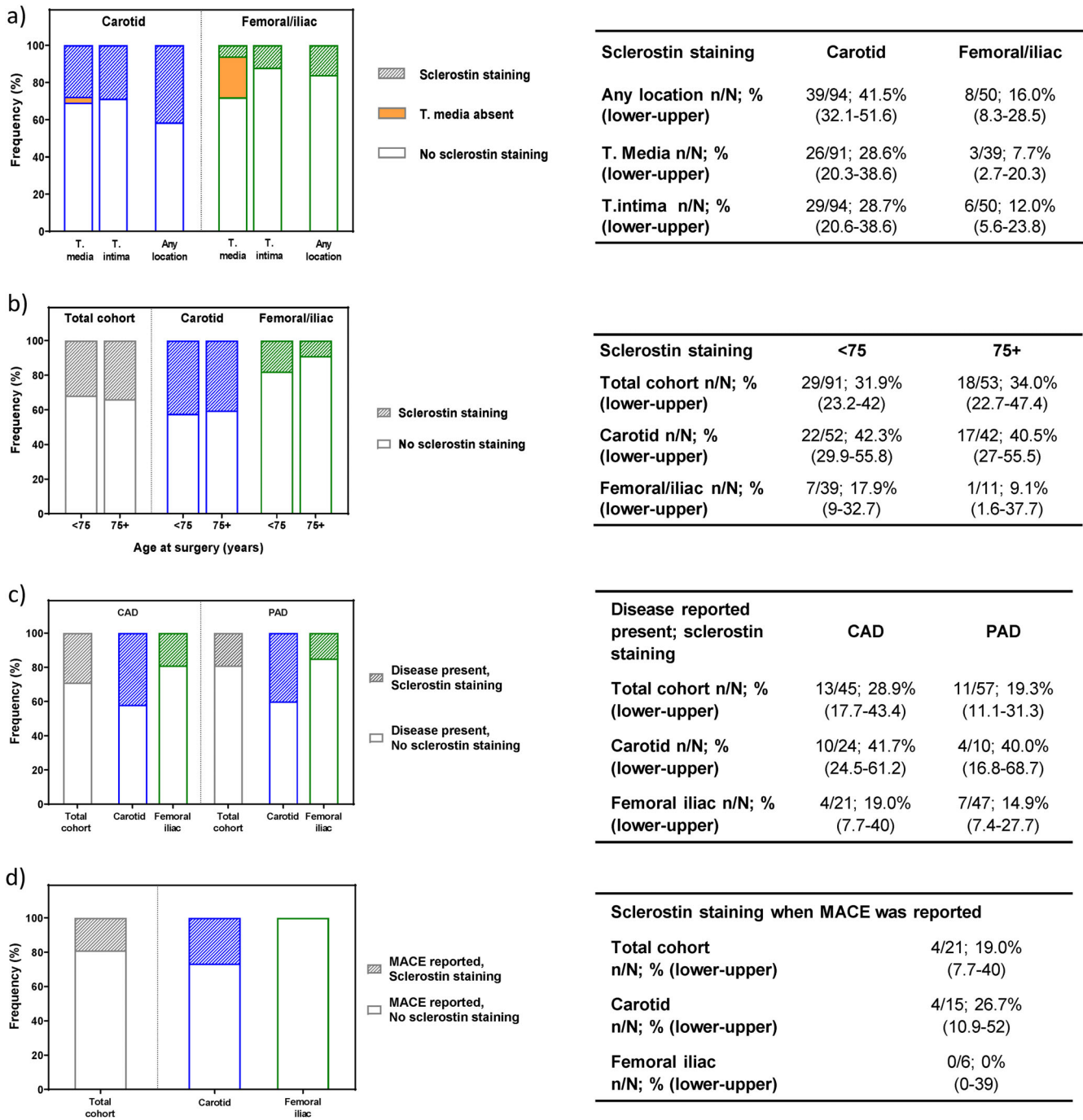


Fig 2. Frequency of sclerostin staining in human AS plaques and association with patient characteristics. (A) Frequency of sclerostin staining by plaque anatomical origin ($n = 94$ carotid; $n = 50$ femoral/iliac) and location within the plaque. (B) Frequency of sclerostin staining by patient age, stratified as younger than 75 years ($n = 91$) or 75 years and older ($n = 53$), for plaques collected from any anatomical location or by carotid or femoral/iliac artery subgroups. (C) Frequency of sclerostin staining in cohort with a history of coronary artery disease (CAD; $n = 45$) or peripheral artery disease (PAD; $n = 57$) before endarterectomy, shown for all plaques and further stratified by anatomical origin of the plaque. (D) Frequency of sclerostin staining in subgroup of the total cohort in whom major adverse cardiovascular event (MACE) occurred within the 3-year follow-up period ($n = 21$). Graphs are presented as stacked histograms (shaded bar indicates positive sclerostin staining; empty bar indicates absent sclerostin staining; orange solid bar indicates plaques for which T. media was not present and hence staining of this region could not be scored). Tabulated summaries to the right of each graph present number of positive sclerostin staining (n) within the cohort (N), percent of positive sclerostin staining within that group with 95% confidence interval shown in brackets.

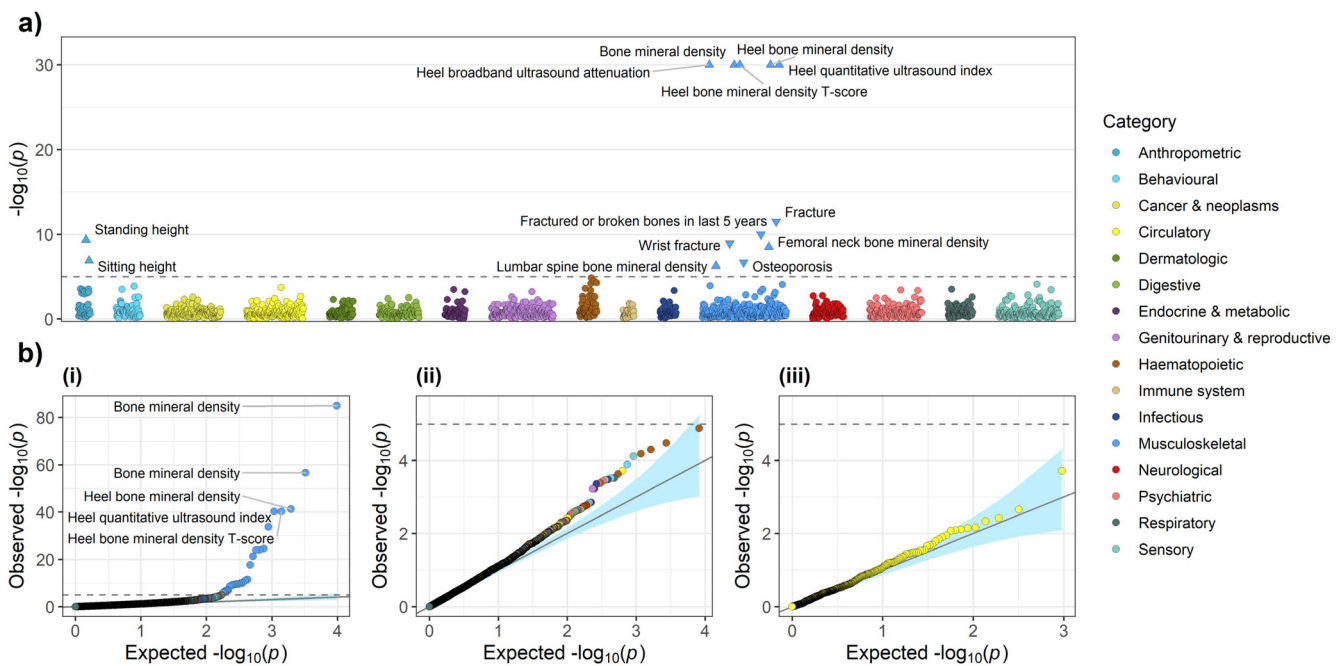


Fig 3. Phenomewide association study (PheWAS) of variants associated with reduced *SOST* expression (rs9899889, rs1107748, and rs66838809). (A) PheWAS plot of the minimum p value across the three variants for each phenotype (number of phenotypes tested = 1706). (B) Quantile-quantile plots for: (i) all associations, (ii) all non-skeletal-related associations (ie, associations not in the anthropometric and musculoskeletal phenotype categories), and (iii) circulatory associations only. Phenotypes were grouped into phenotypic categories. The dashed gray horizontal line indicates a Bonferroni-adjusted p value threshold of $0.05/n_{tests} = 0.05/4887 \approx 1.0 \times 10^{-5}$. Directions of effect for those associations that surpass this threshold are indicated in the PheWAS plot by the direction in which the triangle is pointing. The light blue shaded areas on the quantile-quantile plots represent 95% confidence intervals. The PheWAS plot y-axis was truncated to $-\log_{10}(p) = 30$. Bone mineral density was estimated using heel ultrasound. Note: The triglyceride, high-density lipoprotein cholesterol and apolipoprotein A results for rs9899889 were replaced with those adjusted for rs72836561 in the *CD300LG* gene (Supplemental Table S6).

the 95% confidence interval (94.2% of the associations fall within the confidence interval) in the quantile-quantile plot (Fig. 3B(iii)). The circulatory associations are similar to those for all non-skeletal body systems, as shown in Fig. 3B(ii) and are in marked contrast to the significant musculoskeletal associations shown in Fig. 3B(i), where many associations clearly exceed the dotted line showing the Bonferroni p value threshold $\approx 1 \times 10^{-5}$.

Combining effects across these variants (see Materials and Methods for meta-analysis approach accounting for correlation between variants) for cardiovascular endpoints, including coronary artery disease, myocardial infarction, and stroke, we found no evidence of association (all p values $>.05$; Bonferroni p value threshold of $0.05/18$ cardiovascular endpoints or risk factors = 0.0028 ; Fig. 4A). Similarly, we found no evidence of association with cardiovascular risk factors, including body mass index, systolic or diastolic blood pressure, low- or high-density lipoprotein cholesterol, or triglycerides (after accounting for the effects of the *CDL300LG* gene), after correcting for multiple testing (Fig. 4B). Further inspection of variants in the region surrounding *SOST* for the major cardiovascular endpoints also showed no evidence of genetic associations with these phenotypes (Supplemental Fig. S6).

We assessed two further variants remote from *SOST* that are associated with reduced circulating sclerostin protein levels in *trans*⁽³⁵⁾ (rs215226, located on chromosome 12 in *B4GALNT3*; rs7241221, located on chromosome 18 next to *GALNT1*); no *cis* variants were associated with circulating protein levels of sclerostin. These alleles were also associated with increased BMD and other musculoskeletal and anthropometric phenotypes but

were not associated with any cardiovascular phenotypes (Supplemental Fig. S7 and Supplemental Table S7).

Sensitivity analyses using genetic variants associated with BMD in the *SOST* region

Recently, Bovijn and colleagues performed a similar set of genetic analyses using variants in the *SOST* region associated with BMD, rs7209826 and rs188810925,⁽³⁶⁾ and suggested that genetic inhibition of sclerostin could potentially elevate cardiovascular risk.⁽⁷⁶⁾ Both variants are correlated with the variants selected above: rs7209826 with rs1107748 $r^2 = 0.707$ and rs188810925 with rs66838809 $r^2 = 0.888$. For completeness, these variants were also analyzed in the current work, and the results were consistent with the variant set already described here; namely, the variants showed positive associations with increased BMD phenotypes but no associations with any cardiovascular-related phenotypes (Supplemental Fig. S8 and Table S8). One further additional set of variants in the *SOST* region associated with BMD, rs2741856 and rs7217502⁽³²⁾ (both variants are correlated with the variants selected above: rs7217502 with rs1107748 $r^2 = 0.689$ and rs2741856 with rs66838809 $r^2 = 0.579$), were also analyzed and yielded results consistent with all other variants studied (Supplemental Fig. S9 and Supplemental Table S9).

The main inferences made in Bovijn and colleagues are based on a set of fixed-effects meta-analyses, which assume that rs7209826 and rs188810925 are independent. However, these

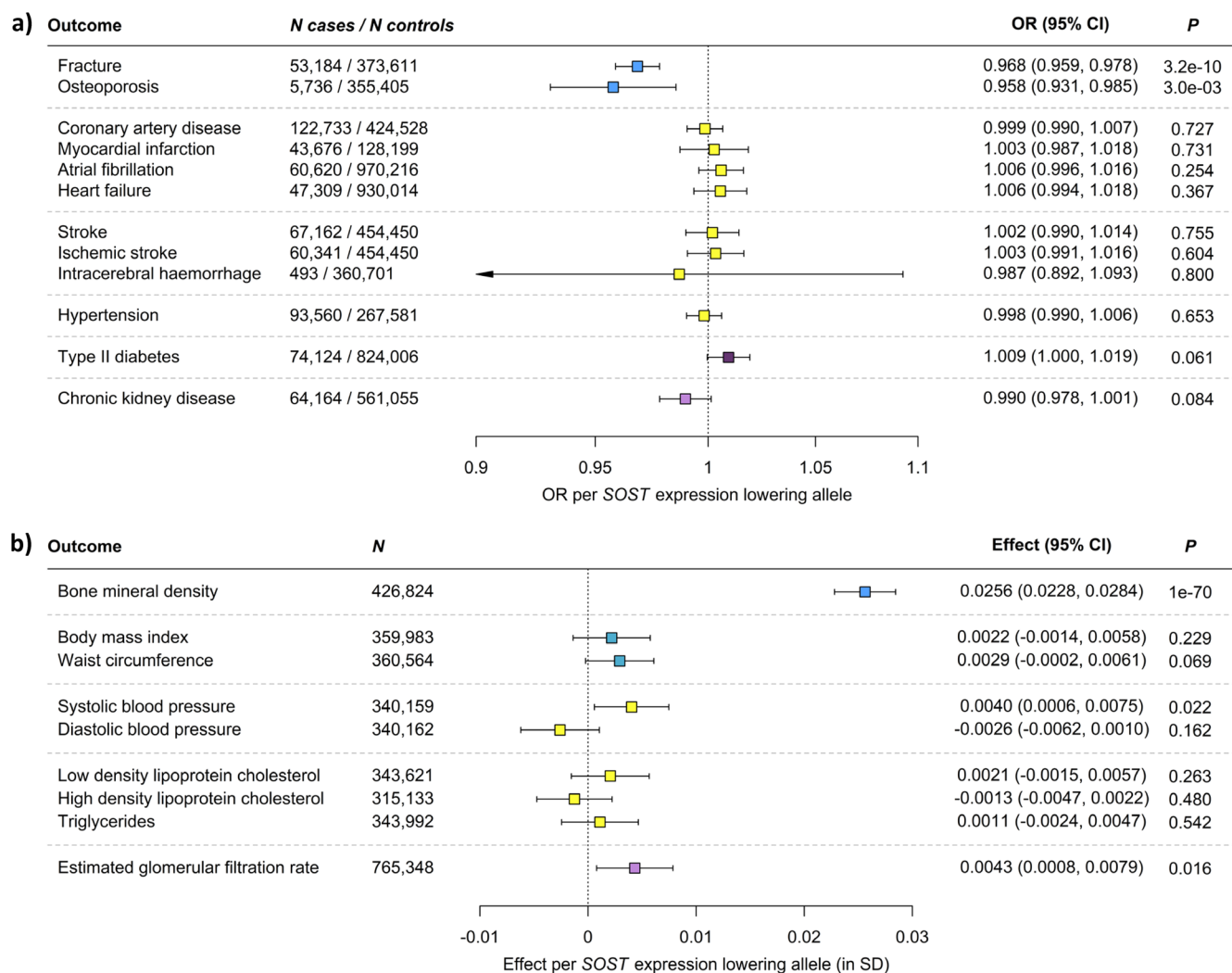


Fig 4. Meta-analysis of variants associated with reduced *SOST* expression and cardiovascular disease endpoints and risk factors. (A) Associations with disease endpoints. (B) Associations with bone mineral density and cardiovascular risk factors. Boxes represent point estimates of effects in odds ratio (OR) (A) or standard deviation (SD) (B) units. Lines represent 95% confidence intervals. The box coloring scheme is the same as that used in Fig. 1. Since we tested 18 cardiovascular endpoints and risk factors, we used a Bonferroni-adjusted p value threshold of $0.05/n_{tests} = 0.05/18 = 0.0028$. Bone mineral density was estimated using heel ultrasound. Note: The triglyceride and high-density lipoprotein cholesterol results for rs9899889 were replaced with those adjusted for rs72836561 in the *CD300LG* gene (Supplemental Table S6). The number of samples (n) per outcome is shown within each panel.

variants are correlated ($r^2 = 0.124$, $D' = 1$, $p = 6.7 \times 10^{-29}$), leading to overly precise results and underestimated p values. We re-performed their primary analysis of cardiovascular disease events, taking into account the correlation between the two variants (see Materials and Methods), and using Bovijn and colleagues' Bonferroni threshold of 0.004 (main cardiovascular events and risk factors), there is no evidence of association (Supplemental Fig. S10; MI and/or coronary revascularization $p = .011$, coronary heart disease [CHD] $p = .078$, MACE $p = .019$).

Discussion

This study applied a dual approach to search for potential associations between sclerostin expression in the vasculature and serious cardiovascular events. Atherosclerosis is a driver of most myocardial infarctions and many strokes,⁽¹⁸⁾ which are a subset

of MACE events. First, immunohistochemistry was used in a focused cross-sectional study to examine local sclerostin expression in FFPE specimens of well-phenotyped AS plaques archived in the AtheroExpress biobank.⁽²⁵⁾ Sclerostin was observed in normal aorta, which was used as a positive control tissue in this study. Although the primary aim of this study was not to compare sclerostin staining intensity in plaques and aorta, it was notable that staining of AS plaques, when observed, was of lower intensity than the aorta control tissues. Across the 144 plaques examined, immunoreactivity was low or absent and most showed no staining. Where present, sclerostin staining was restricted to deeper parts of the plaque/vessel wall (T. media and immediate adjacent subintimal region distant from the lumen). In line with these findings, *SOST* downregulation was reported in human AS plaques compared with aorta⁽⁷⁷⁾ and *SOST* expression in the aorta is reduced in rabbit and mouse models of atherosclerosis.^(16,78) Sclerostin protein has been detected in

human aorta⁽⁸⁾ and in the radial artery of patients with advanced chronic kidney disease.⁽¹⁴⁾

Importantly, sclerostin staining was not observed in areas relevant to plaque stability or plaque rupture (ie, superficial region, fibrous cap, endothelial cells). The nature and characteristics of AS plaques are linked to thrombotic events,^(23,64) and the association of plaque characteristics with clinical events for samples within the AtheroExpress biobank has previously been assessed.^(79,80) The plaques included in the current study were not selected based on potential associations with plaque characteristics or clinical events, and the outcomes in our data set were in line with previously reported associations. Sclerostin immunoreactivity was not associated with intraplaque hemorrhage, lipid content, smooth muscle cells, or collagen. The inverse association between sclerostin staining and dystrophic calcification of the acellular necrotic core in advanced plaques most likely reflects a passive process of dystrophic mineralization rather than being an active, cell-mediated or transcriptionally regulated process.^(81,82) Sclerostin staining was also not associated with age at endarterectomy, history of arterial disease prior to, or MACE during the patient follow-up period (minimum 3 years), although the total number of sclerostin-positive plaques was also low, which decreased the power to examine associations between sclerostin expression and plaque or patient clinical histories/outcomes. Finally, sclerostin immunoreactivity was not associated with expression of the pro-inflammatory cytokines MCP1, IL6, and TNF α or with osteopontin, a biomarker of cardiovascular events.⁽⁶⁵⁾ Based on these findings, it is difficult to postulate a mechanism to explain how sclerostin or its inhibition would have any direct effect on plaque stability.

There are some limitations to this part of the study. Although IHC is an ideal technique to examine the location of target protein expression, it is less suited to protein quantitation; hence, findings from the current study were qualitative. Although the staining protocol had been optimized to achieve maximal sensitivity while retaining specificity, sclerostin immunoreactivity was constrained by the limit of detection of this platform. The absence of sclerostin staining in the superficial T. intima or endothelium indicates sclerostin was not produced in this region of the plaque. Sclerostin is a negative regulator of Wnt signaling, which occurs locally in an autocrine/paracrine fashion.⁽⁸³⁾ The heparin-binding domain of sclerostin should diminish the potential for its diffusion from deep in the plaque toward the lumen⁽⁸⁴⁾ and the absence of staining suggests any such amount was low. The objective of this part of the study was to investigate the extent and location of sclerostin expression in human AS plaques; however, confirmation of the presence of a protein does not inform on its function in that location. In preclinical studies, transcriptomic analysis indicated that sclerostin inhibition did not affect Wnt pathways in the vasculature in the presence or absence of atherosclerosis.⁽¹⁶⁾ Application of more sensitive techniques such as mass spectroscopy proteomics and single-cell RNA sequencing could be usefully applied in future studies to further investigate sclerostin expression in human AS plaques and understand its functional relevance. Finally, no insights into temporal aspects of sclerostin expression with atheroprotection were gained from this work, although progressive attenuation of *SOST* expression with atheroprotection was reported in a mouse model.⁽⁶⁸⁾

Immunohistochemistry can yield false-positive results. A recent report described IHC staining of sclerostin in AS plaques from patients who underwent carotid endarterectomy.⁽⁸⁵⁾ In contrast to our findings, Leto and colleagues used a commercially available

rabbit polyclonal sclerostin antibody from Abcam and detected sclerostin expression in the entire set of 46 plaques examined, noting immunopositivity in the T. media and core of the plaque, infiltrating macrophages, and VSMC. This discrepancy may reflect differences in antibody specificity. In the present study, great care was taken to ensure sclerostin staining was highly specific and sensitive. Comparison of four sclerostin antibodies, including two commercially available rabbit polyclonals from Abcam, highlighted the importance of antibody validation, staining optimization, and inclusion of negative control tissues in IHC studies. Unlike the highly specific Scl-Ab #1, which showed no immunoreactivity in tissues known not to express sclerostin protein (ie, kidney and liver), the commercial reagents exhibited intense staining in both liver and kidney, which suggests non-specific binding (Supplemental Fig. S1) and may account for the apparent widespread “sclerostin” immunoreactivity in atherosclerotic plaques observed by Leto and colleagues.⁽⁸⁵⁾

Population level human genetic data can be highly informative in predicting the pharmacological effects of perturbing a drug target, revealing mechanisms of action, identifying alternate indications, and predicting adverse drug events.⁽⁸⁶⁾ To explore whether lowering of sclerostin levels was associated with increased lifetime cardiovascular risk, a comprehensive PheWAS was performed to assess the phenotypic effects of genetic variation simultaneously across thousands of phenotypes from large-scale studies (including UK Biobank, $N = 361,194$). Variants associated with reduced *SOST* expression and increased BMD acted as a proxy for the pharmacological outcome of sclerostin inhibition, albeit reflecting lifelong effects rather than mimicking a defined period of treatment to neutralize sclerostin function in a clinical setting.

Here, three different approaches were employed to select *SOST*-related variants for exploration of their association with bone physiology and cardiovascular phenotypes: (i) variants associated with decreased arterial mRNA *SOST* expression and increased BMD; (ii) variants remote from the *SOST* region associated with decreased circulating sclerostin protein (ie, *trans* acting variants); and (iii) variants in the *SOST* region associated with increased BMD. The results were consistent: *SOST* variants associated with reduced sclerostin expression were associated with increased BMD and reduced risk of fracture and osteoporosis but were not associated with an increased lifetime risk of any cardiovascular outcomes, including MI, stroke, coronary artery disease, atrial fibrillation, and heart failure or with traits associated with a higher risk such as hypertension and type II diabetes.

The only cardiovascular-related traits showing any association with variants at the *SOST* locus were circulating triglyceride and HDL levels. This association has been reported multiple times previously and attributed to a nearby gene, *CD300LG*,^(68–75) approximately 100 kb upstream of the *SOST* gene. A functional missense variant in *CD300LG* (rs72836561, Arg82Cys) drives the associations in this region.⁽⁷³⁾ After adjusting for the effects of the *CD300LG* gene on triglyceride and HDL levels, there was no evidence of associations with CV traits by more than would be expected by chance. Indeed, when effects across the *SOST* variants were combined, there was no evidence of associations for the major CV endpoints nor with any CV risk factors. *SOST* regional association plots (Supplemental Fig. S6) for the CV endpoints also display the lack of association between variants in this region of the genome with these phenotypes. When the PheWAS analysis was extended to include a range of phenotypic traits across different body systems, there was no evidence that the *SOST* variants were associated with any phenotype other

than the expected musculoskeletal and BMD traits (Fig. 3 and Supplemental Figs. S7, S8, and S9). This consistent lack of association between CV risk and lowered sclerostin using a range of *SOST* variants is compelling because these analyses reflect a lifetime of reduced sclerostin. Consistent with the absence of association between reduced *SOST* expression and CV risk factors in this study, there were no reports of hypertension or alteration in blood pressure, glucose control, or lipids, based on treatment-emergent adverse events in clinical trials with the sclerostin antibody romosozumab;⁽⁸⁷⁾ similarly, there were no clinically relevant changes in blood pressure, heart rate, or electrocardiogram parameters during treatment with a second sclerostin antibody, blosozumab.⁽⁸⁸⁾ In nonclinical studies, there was no evidence of an association between sclerostin inhibition and blood pressure, heart rate, or electrocardiograms, and romosozumab or recombinant sclerostin did not elicit vasoconstriction in human coronary rings.⁽¹⁶⁾ Within the same report, no functional morphologic or transcriptional effects on the cardiovascular system were observed in animal models in the presence or absence of atherosclerosis.

A recent study using similar approaches with two *SOST* variants suggested genetic inhibition of sclerostin could potentially elevate cardiovascular risk.⁽⁷⁶⁾ It was of interest to understand why the outcome of that analysis differed from the one presented here. Bovijn and colleagues treated their selected variants as if they were independent of each other; however, these variants are correlated ($p = 6.7 \times 10^{-29}$). This non-independence inflated the precision of associations on all phenotypes studied and underestimated p values. Indeed, upon accounting for this correlation and applying a Bonferroni correction for multiple testing, the results for their primary CV disease endpoints were no longer statistically significant (Supplemental Fig. S10). There were also directional discrepancies in the cardiovascular endpoints between biobanks in the supplementary materials of that publication,⁽⁴⁾ although these could be attributable to low power in some of these analyses.

The genetics approaches in the current study reflect a risk of CV outcomes resulting from a lifetime of genetically lowered sclerostin levels. The ability to extrapolate these findings to inform on the potential outcomes after therapeutic inhibition of sclerostin is complicated by the relatively short duration of treatment with a sclerostin-neutralizing antibody in the management of osteoporosis (12 months in the case of romosozumab). This is inherent to any study using germline variants as a proxy for pharmacological interventions with significantly shorter observation periods.⁽⁸⁶⁾ CV risk gradually increases with age, with an approximately linear increase in risk for each additional decade of life;⁽⁶⁰⁾ thus, the genetics approaches may overestimate the impact of reduced sclerostin.

In addition, the variants associated with reduced circulating sclerostin protein were in *trans*, and while *trans*-acting effects of variants affecting expression of genes on other chromosomes have been reported,⁽⁸⁹⁾ further validation of the relationship between these associations and *SOST* is required. Nonetheless, although these variants were associated with increased BMD and other musculoskeletal and anthropometric phenotypes, there was still no evidence of an association between the two *trans* variants assessed and cardiovascular risk.

The approaches used here utilized common genetic variants. Rare *SOST* variants causing sclerosteosis and van Buchem disease^(2,3,90) can also inform on the consequence of absent/reduced sclerostin. Sclerosteosis patients typically have a shortened life span, largely reflecting complications arising from raised intracranial pressure, but at least five have lived for more

than 50 years without reported CV effects. Van Buchem patients have a normal life span. There are no reports of CV effects in sclerosteosis or van Buchem patients and no mention of CV issues in a published clinical management plan.^(91,92)

In summary, the data generated from these two independent investigations did not support a mechanistic link between sclerostin expression (or its inhibition) in the vasculature and cardiovascular-related outcomes. In a small focused cross-sectional study that examined sclerostin presence local to AS plaques, there was a lack of sclerostin expression in the fibrous cap and luminal endothelium in human arterial atherosclerotic plaques—key sites related to the pathophysiology of plaque rupture and erosion⁽⁹³⁾—and a lack of any relationship between sclerostin immunoreactivity and morphological characteristics or biomarkers associated with cardiovascular events. Population-based genetic analyses using common variants associated with reduced expression of the *SOST* gene indicated that natural genetic modulation of *SOST* by variants with a significant positive effect on musculoskeletal readouts, including bone physiology, had no significant effect on cardiovascular-related outcomes.

Disclosures

This study was funded by UCB Pharma and Amgen Inc. GH, JRS, PH, CV, RO, MA, and AW are employees of UCB Pharma and may hold stock/stock awards. RB and JRT are/have been employees of Amgen Inc. and may hold stock/stock awards. GP has previously served on an Advisory Board for Amgen Inc.

Acknowledgments

The authors thank Dr Chris Paszty (Amgen Inc.) and Dr Jochen Dunkel (UCB Pharma) for their helpful support, and Petra van der Kraak (University Medical Centre Utrecht) for technical support to perform IHC staining of AS plaques. Summary statistics were downloaded from the NHGRI-EBI GWAS Catalog⁽⁴⁸⁾ for studies GCST006979, GCST006980,⁽³²⁾ GCST005194,⁽⁴⁶⁾ GCST005838, GCST005843,⁽⁴²⁾ GCST006414,⁽⁴³⁾ GCST009541,⁽⁴⁵⁾ GCST007517,⁽⁴¹⁾ GCST008058, and GCST008064,⁽⁴⁷⁾ downloaded on June 25, 2020. Data on coronary artery disease and myocardial infarction have been contributed by CARDIoGRAMplusC4D investigators and have been downloaded from www.cardiogramplusc4d.org. The MEGASTROKE project received funding from sources specified at <http://www.megastroke.org/acknowledgments.html>. We thank the MEGASTROKE authors; the author list is available at <https://www.megastroke.org/authors.html>. All summary genetic association results used are available in the public domain.

Authors' roles: GH, PH, RO, RWB, JRT and GP: conceptualization and methodology for IHC study. RO: Scl-Ab investigations. PH, IVK, GH, and GP: formal analysis of IHC study data. GH, JRS, CV, AW, and MA: conceptualization for genetics analysis. JRS and CV: investigation and formal analysis for human genetic association studies. GH, JRS, PH, CV, and AW: original draft preparation. All co-authors reviewed and edited the final version of the submitted manuscript.

Author contributions: GH: Conceptualization; formal analysis; methodology; writing-original draft; writing-review & editing. JRS: Conceptualization; formal analysis; investigation; writing-original draft; writing-review & editing. PH: Conceptualization; formal analysis; methodology; writing-original draft; writing-review & editing. IVK: Formal analysis; writing-review & editing.

CV: Conceptualization; formal analysis; investigation; writing-original draft; writing-review & editing. RO: Investigation; writing-review & editing. RWB: Conceptualization; methodology; writing-review & editing. JT: Conceptualization; methodology; writing-review & editing. MA: Formal analysis; writing-review & editing. AW: Formal analysis; writing-original draft; writing-review & editing. GP: Conceptualization; formal analysis; methodology; writing-review & editing.

Data availability statement

The genetics data was publicly available. Other datasets generated during and/or analysed during this study which are not publicly available or included as supplementary files are available from the corresponding author on reasonable request.

References

1. Holdsworth G, Roberts SJ, Ke HZ. Novel actions of sclerostin on bone. *J Mol Endocrinol*. 2019;62(2):R167-R185.
2. Balemans W, Ebeling M, Patel N, et al. Increased bone density in sclerosteosis is due to the deficiency of a novel secreted protein (SOST). *Hum Mol Genet*. 2001;10(5):537-543.
3. Brunkow ME, Gardner JC, Van Ness J, et al. Bone dysplasia sclerosteosis results from loss of the SOST gene product, a novel cystine knot-containing protein. *Am J Hum Genet*. 2001;68(3):577-589.
4. Poole KE, van Bezooijen RL, Loveridge N, et al. Sclerostin is a delayed secreted product of osteocytes that inhibits bone formation. *FASEB J*. 2005;19(13):1842-1844.
5. McClung MR. Sclerostin antibodies in osteoporosis: latest evidence and therapeutic potential. *Ther Adv Musculoskelet Dis*. 2017;9(10):263-270.
6. McClung MR. Romosozumab for the treatment of osteoporosis. *Osteoporos Sarcopenia*. 2018;4(1):11-15.
7. Chouinard L, Felx M, Mellal N, et al. Carcinogenicity risk assessment of romosozumab: a review of scientific weight-of-evidence and findings in a rat lifetime pharmacology study. *Regul Toxicol Pharmacol*. 2016;81:212-222.
8. Didangelos A, Yin X, Mandal K, Baumert M, Jahangiri M, Mayr M. Proteomics characterization of extracellular space components in the human aorta. *Mol Cell Proteomics*. 2010;9(9):2048-2062.
9. Krishna SM, Seto SW, Jose RJ, et al. Wnt signaling pathway inhibitor sclerostin inhibits angiotensin II-induced aortic aneurysm and atherosclerosis. *Arterioscler Thromb Vasc Biol*. 2017;37(3):553-566.
10. Brandenburg VM, Kramann R, Koos R, et al. Relationship between sclerostin and cardiovascular calcification in hemodialysis patients: a cross-sectional study. *BMC Nephrol*. 2013;14:219.
11. Koos R, Brandenburg V, Mahnken AH, et al. Sclerostin as a potential novel biomarker for aortic valve calcification: an in-vivo and ex-vivo study. *J Heart Valve Dis*. 2013;22(3):317-325.
12. Kramann R, Brandenburg VM, Schurgers LJ, et al. Novel insights into osteogenesis and matrix remodelling associated with calcific uraemic arteriopathy. *Nephrol Dial Transplant*. 2013;28(4):856-868.
13. Rukov JL, Gravesen E, Mace ML, et al. Effect of chronic uremia on the transcriptional profile of the calcified aorta analyzed by RNA sequencing. *Am J Physiol Renal Physiol*. 2016;310(6):F477-F491.
14. Zhou H, Yang M, Li M, Cui L. Radial artery sclerostin expression in chronic kidney disease stage 5 predialysis patients: a cross-sectional observational study. *Int Urol Nephrol*. 2017;49(8):1433-1437.
15. Zhu D, Mackenzie NC, Millan JL, Farquharson C, MacRae VE. The appearance and modulation of osteocyte marker expression during calcification of vascular smooth muscle cells. *PLoS One*. 2011;6(5).
16. Turk JR, Deaton AM, Yin J, et al. Nonclinical cardiovascular safety evaluation of romosozumab, an inhibitor of sclerostin for the treatment of osteoporosis in postmenopausal women at high risk of fracture. *Regul Toxicol Pharmacol*. 2020;115:104697.
17. Saag KG, Petersen J, Brandi ML, et al. Romosozumab or alendronate for fracture prevention in women with osteoporosis. *N Engl J Med*. 2017;377(15):1417-1427.
18. Libby P, Buring JE, Badimon L, et al. Atherosclerosis. *Nat Rev Dis Primers*. 2019;5(1):56.
19. Lanza GA, Careri G, Crea F. Mechanisms of coronary artery spasm. *Circulation*. 2011;124(16):1774-1782.
20. Thygesen K, Alpert JS, Jaffe AS, et al. Fourth universal definition of myocardial infarction (2018). *Circulation*. 2018;138(20):e618-e651.
21. Kubo T, Imanishi T, Takarada S, et al. Assessment of culprit lesion morphology in acute myocardial infarction: ability of optical coherence tomography compared with intravascular ultrasound and coronary angiography. *J Am Coll Cardiol*. 2007;50(10):933-939.
22. Farb A, Burke AP, Tang AL, et al. Coronary plaque erosion without rupture into a lipid core. A frequent cause of coronary thrombosis in sudden coronary death. *Circulation*. 1996;93(7):1354-1363.
23. Pasterkamp G, den Ruijter HM, Libby P. Temporal shifts in clinical presentation and underlying mechanisms of atherosclerotic disease. *Nat Rev Cardiol*. 2017;14(1):21-29.
24. van Lammeren GW, den Ruijter HM, Vrijenhoek JE, et al. Time-dependent changes in atherosclerotic plaque composition in patients undergoing carotid surgery. *Circulation*. 2014;129(22):2269-2276.
25. Verhoeven BA, Velema E, Schoneveld AH, et al. Athero-express: differential atherosclerotic plaque expression of mRNA and protein in relation to cardiovascular events and patient characteristics. *Rationale and design*. *Eur J Epidemiol*. 2004;19(12):1127-1133.
26. Pendergrass SA, Brown-Gentry K, Dudek SM, et al. The use of phenome-wide association studies (PheWAS) for exploration of novel genotype-phenotype relationships and pleiotropy discovery. *Genet Epidemiol*. 2011;35(5):410-422.
27. Price AL, Spencer CC, Donnelly P. Progress and promise in understanding the genetic basis of common diseases. *Proc Biol Sci*. 2015;282(1821):20151684.
28. Holmes MV. Human genetics and drug development. *N Engl J Med*. 2019;380(11):1076-1079.
29. Walker VM, Davey Smith G, Davies NM, Martin RM. Mendelian randomization: a novel approach for the prediction of adverse drug events and drug repurposing opportunities. *Int J Epidemiol*. 2017;46(6):2078-2089.
30. GTEx Consortium. Human genomics. The genotype-tissue expression (GTEx) pilot analysis: multitissue gene regulation in humans. *Science*. 2015;348(6235):648-660.
31. Dudbridge F, Gusnanto A. Estimation of significance thresholds for genomewide association scans. *Genet Epidemiol*. 2008;32(3):227-234.
32. Morris JA, Kemp JP, Youlten SE, et al. An atlas of genetic influences on osteoporosis in humans and mice. *Nat Genet*. 2019;51(2):258-266.
33. Machiela MJ, Chanock SJ. LDlink: a web-based application for exploring population-specific haplotype structure and linking correlated alleles of possible functional variants. *Bioinformatics*. 2015;31(21):3555-3557.
34. 1000 Genomes Project Consortium, Auton A, Brooks LD, et al. A global reference for human genetic variation. *Nature*. 2015;526(7571):68-74.
35. Zheng J, Maerz W, Gergei I, et al. Mendelian randomization analysis reveals a causal influence of circulating sclerostin levels on bone mineral density and fractures. *J Bone Miner Res*. 2019;34(10):1824-1836.
36. Kemp JP, Morris JA, Medina-Gomez C, et al. Identification of 153 new loci associated with heel bone mineral density and functional involvement of GPC6 in osteoporosis. *Nat Genet*. 2017;49(10):1468-1475.
37. Barrett JC, Fry B, Maller J, Daly MJ. Haploview: analysis and visualization of LD and haplotype maps. *Bioinformatics*. 2005;21(2):263-265.
38. Sudlow C, Gallacher J, Allen N, et al. UKbiobank: an open access resource for identifying the causes of a wide range of complex diseases of middle and old age. *PLoS Med*. 2015;12(3):e1001779.

39. Kamat MA, Blackshaw JA, Young R, et al. PhenoScanner V2: an expanded tool for searching human genotype-phenotype associations. *Bioinformatics*. 2019;35(22):4851-4853.
40. Staley JR, Blackshaw J, Kamat MA, et al. PhenoScanner: a database of human genotype-phenotype associations. *Bioinformatics*. 2016;32(20):3207-3209.
41. Mahajan A, Taliun D, Thurner M. Fine-mapping type 2 diabetes loci to single-variant resolution using high-density imputation and islet-specific epigenome maps. *Nat Genet*. 2018;50(11):1505-1513.
42. Malik R, Chauhan G, Traylor M, et al. Multiancestry genome-wide association study of 520,000 subjects identifies 32 loci associated with stroke and stroke subtypes. *Nat Genet*. 2018;50(4):524-537.
43. Nielsen JB, Thorolfsdottir RB, Fritsche LG, et al. Biobank-driven genomic discovery yields new insight into atrial fibrillation biology. *Nat Genet*. 2018;50(9):1234-1239.
44. Nikpay M, Goel A, Won HH, et al. A comprehensive 1,000 Genomes-based genome-wide association meta-analysis of coronary artery disease. *Nat Genet*. 2015;47(10):1121-1130.
45. Shah S, Henry A, Roselli C, et al. Genome-wide association and Mendelian randomisation analysis provide insights into the pathogenesis of heart failure. *Nat Commun*. 2020;11(1):163.
46. van der Harst P, Verweij N. Identification of 64 novel genetic loci provides an expanded view on the genetic architecture of coronary artery disease. *Circ Res*. 2018;122(3):433-443.
47. Wuttke M, Li Y, Li M, et al. A catalog of genetic loci associated with kidney function from analyses of a million individuals. *Nat Genet*. 2019;51(6):957-972.
48. Buniello A, MacArthur JAL, Cerezo M, et al. The NHGRI-EBI GWAS catalog of published genome-wide association studies, targeted arrays and summary statistics 2019. *Nucleic Acids Res*. 2019;47(D1):D1005-D1012.
49. Hemani G, Zheng J, Elsworth B, et al. The MR-base platform supports systematic causal inference across the human phenome. *Elife*. 2018;7:e34408. Available at: <https://doi.org/10.7554/eLife.34408>.
50. Bulik-Sullivan B, Finucane HK, Anttila V, et al. An atlas of genetic correlations across human diseases and traits. *Nat Genet*. 2015;47(11):1236-1241.
51. Yang J, Ferreira T, Morris AP, et al. Conditional and joint multiple-SNP analysis of GWAS summary statistics identifies additional variants influencing complex traits. *Nat Genet*. 2012;44(4):369-375 S1-3.
52. Burgess S, Dudbridge F, Thompson SG. Combining information on multiple instrumental variables in Mendelian randomization: comparison of allele score and summarized data methods. *Stat Med*. 2016;35(11):1880-1906.
53. Suderman M, Staley JR, French R, Arathimos R, Simpkin A, Tilling K. dmrrf: identifying differentially methylated regions efficiently with power and control. *bioRxiv*. 2018:508556. Available at: <https://doi.org/10.1101/508556>.
54. Chen SY, Feng Z, Yi X. A general introduction to adjustment for multiple comparisons. *J Thorac Dis*. 2017;9(6):1725-1729.
55. Mitchell R, Elsworth BL, Mitchell R, et al. MRC IEU UK Biobank GWAS pipeline version 2. University of Bristol; 2019.
56. McKinney W. Data structures for statistical computing in Python. 2010.
57. Wickham H. ggplot2: elegant graphics for data analysis. Houston, TX: Springer International Publishing; 2016.
58. Viechtbauer W. Conducting meta-analyses in R with the metafor package. 2010;36(3):48.
59. Li H. Tabix: fast retrieval of sequence features from generic TAB-delimited files. *Bioinformatics*. 2011;27(5):718-719.
60. Marma AK, Lloyd-Jones DM. Systematic examination of the updated Framingham heart study general cardiovascular risk profile. *Circulation*. 2009;120(5):384-390.
61. North BJ, Sinclair DA. The intersection between aging and cardiovascular disease. *Circ Res*. 2012;110(8):1097-1108.
62. Vangen-Lonne AM, Wilsgaard T, Johnsen SH, Carlsson M, Mathiesen EB. Time trends in incidence and case fatality of ischemic stroke: the Tromso study 1977-2010. *Stroke*. 2015;46(5):1173-1179.
63. Hellings WE, Moll FL, de Kleijn DP, Pasterkamp G. 10-years experience with the Athero-express study. *Cardiovasc Diagn Ther*. 2012;2(1):63-73.
64. van Koevorden ID, Vrijenhoek JE, de Borst GJ, den Ruijter HM, Pasterkamp G. Biobanking in carotid artery disease: translation to clinical practice. *J Cardiovasc Surg (Torino)*. 2017;58(2):178-186.
65. de Kleijn DP, Moll FL, Hellings WE, et al. Local atherosclerotic plaques are a source of prognostic biomarkers for adverse cardiovascular events. *Arterioscler Thromb Vasc Biol*. 2010;30(3):612-619.
66. Cosman F, Crittenden DB, Adachi JD, et al. Romosozumab treatment in postmenopausal women with osteoporosis. *N Engl J Med*. 2016;375(16):1532-1543.
67. Padhi D, Jang G, Stouch B, Fang L, Posvar E. Single-dose, placebo-controlled, randomized study of AMG 785, a sclerostin monoclonal antibody. *J Bone Miner Res*. 2011;26(1):19-26.
68. Albrechtsen A, Grarup N, Li Y, et al. Exome sequencing-driven discovery of coding polymorphisms associated with common metabolic phenotypes. *Diabetologia*. 2013;56(2):298-310.
69. de Vries PS, Brown MR, Bentley AR, et al. Multiancestry genome-wide association study of lipid levels incorporating gene-alcohol interactions. *Am J Epidemiol*. 2019;188(6):1033-1054.
70. Kanoni S, Masca NG, Stirrups KE, et al. Analysis with the exome array identifies multiple new independent variants in lipid loci. *Hum Mol Genet*. 2016;25(18):4094-4106.
71. Klarin D, Damrauer SM, Cho K, et al. Genetics of blood lipids among ~300,000 multi-ethnic participants of the million veteran program. *Nat Genet*. 2018;50(11):1514-1523.
72. Stoy J, Kampmann U, Mengel A, et al. Reduced CD300LG mRNA tissue expression, increased intramyocellular lipid content and impaired glucose metabolism in healthy male carriers of Arg82Cys in CD300LG: a novel genomemetic cross-link between CD300LG and common metabolic phenotypes. *BMJ Open Diabetes Res Care*. 2015;3(1):e000095.
73. Surakka I, Horikoshi M, Magi R, et al. The impact of low-frequency and rare variants on lipid levels. *Nat Genet*. 2015;47(6):589-597.
74. van Leeuwen EM, Sabo A, Bis JC, et al. Meta-analysis of 49 549 individuals imputed with the 1000 Genomes Project reveals an exonic damaging variant in ANGPTL4 determining fasting TG levels. *J Med Genet*. 2016;53(7):441-449.
75. Wang Z, Chen H, Bartz TM, et al. Role of rare and low-frequency variants in gene-alcohol interactions on plasma lipid levels. *Circ Genom Precis Med*. 2020;13(4):e002772.
76. Bovijn J, Krebs K, Chen CY, et al. Evaluating the cardiovascular safety of sclerostin inhibition using evidence from meta-analysis of clinical trials and human genetics. *Sci Transl Med*. 2020;12(549):eaay6570. Available at: <https://doi.org/10.1126/scitranslmed.aay6570>.
77. Sulkava M, Raitoharju E, Levlua M, et al. Differentially expressed genes and canonical pathway expression in human atherosclerotic plaques—Tampere vascular study. *Sci Rep*. 2017;7:41483.
78. Tan L, Wang Z, Li Y. Rabbit models provide insights into bone formation related biological process in atherosclerotic vascular calcification. *Biochem Biophys Res Commun*. 2018;496(4):1369-1375.
79. Derksen WJ, Peeters W, van Lammeren GW, et al. Different stages of intraplaque hemorrhage are associated with different plaque phenotypes: a large histopathological study in 794 carotid and 276 femoral endarterectomy specimens. *Atherosclerosis*. 2011;218(2):369-377.
80. Hellings WE, Peeters W, Moll FL, et al. Composition of carotid atherosclerotic plaque is associated with cardiovascular outcome: a prognostic study. *Circulation*. 2010;121(17):1941-1950.
81. Doherty TM, Asotra K, Fitzpatrick LA, et al. Calcification in atherosclerosis: bone biology and chronic inflammation at the arterial crossroads. *Proc Natl Acad Sci U S A*. 2003;100(20):11201-11206.
82. Schinke T, McKee MD, Karsenty G. Extracellular matrix calcification: where is the action? *Nat Genet*. 1999;21(2):150-151.
83. Nusse R, Clevers H. Wnt/beta-catenin signaling, disease, and emerging therapeutic modalities. *Cell*. 2017;169(6):985-999.
84. Veverka V, Henry AJ, Slocombe PM, et al. Characterization of the structural features and interactions of sclerostin: molecular insight

- into a key regulator of Wnt-mediated bone formation. *J Biol Chem*. 2009;284(16):10890-10900.
85. Leto G, D'Onofrio L, Lucantoni F, et al. Sclerostin is expressed in the atherosclerotic plaques of patients who undergoing carotid endarterectomy. *Diabetes Metab Res Rev*. 2019;35(1):e3069.
86. Diogo D, Tian C, Franklin CS, et al. Phenome-wide association studies across large population cohorts support drug target validation. *Nat Commun*. 2018;9(1):4285.
87. Amgen Inc. Background information for bone, reproductive and urologic drugs advisory committee—biologics license application for romosozumab. 2019.
88. Recker RR, Benson CT, Matsumoto T, et al. A randomized, double-blind phase 2 clinical trial of blosozumab, a sclerostin antibody, in postmenopausal women with low bone mineral density. *J Bone Miner Res*. 2015;30(2):216-224.
89. Bryois J, Buil A, Evans DM, et al. Cis and trans effects of human genomic variants on gene expression. *PLoS Genet*. 2014;10(7):e1004461.
90. Balemans W, Patel N, Ebeling M, et al. Identification of a 52 kb deletion downstream of the SOST gene in patients with van Buchem disease. *J Med Genet*. 2002;39(2):91-97.
91. Appelman-Dijkstra N, Van Lierop A, Papapoulos S. SOST-related sclerosing bone dysplasias. In Adam MP, Ardinger HH, Pagon RA, et al., eds. *GeneReviews*((R)). Seattle, WA: University of Washington; 1993.
92. Hamersma H, Gardner J, Beighton P. The natural history of sclerosteosis. *Clin Genet*. 2003;63(3):192-197.
93. Crea F, Libby P. Acute coronary syndromes: the way forward from mechanisms to precision treatment. *Circulation*. 2017;136(12):1155-1166.